Al-Nahrain Journal of Science
ANJS, Vol. 27(5), December, 2024, pp. 114–122

Preparation and Characterization of Pure Pectin and Silver Loaded Pectin Nanoparticles and their Anticancer Activity

Moayad Rahim Hussein[1,*], Asmaa Hadi Mohammed[2], Farah T. M. Noori[1]

[1]Department of Physics, College of Science, Baghdad University, Baghdad, Iraq
[2]Department of Physics, College of Science, Al-Nahrain University, Jadiriya, Baghdad, Iraq

Article's Information

Received: 03.10.2024
Accepted: 09.12.2024
Published: 15.12.2024

Keywords:
Pectin
Cancer Therapy
AgNPs
AgNPs/pectin

Abstract

A plant-based heteropolysaccharide is recognized for its biocompatibility and biodegradability, making it a promising candidate for green synthesis as a stabilizing agent in the formation of metallic nanostructure. Despite this, Pectin is largely overlooked in the biological industry for MNP (Metallic nanoparticle) production, with no clear reason for its underutilization. A simple and affordable approach for creating Silver Nano products (Ag NPs) has been devised by means of citrus pectin for both a diminishing and stabilizing agent. The Ag NPs have been analyzed through UV-vis, TEM, X-Ray diffraction, and FTIR techniques. The findings revealed that the Ag NPs are spherical, with a consistent, scale of 10 nanometers besides the outstanding dispersion. Moreover, the Ag NPs showed strong anticancer properties. Employing citrus pectin in the synthesis of Ag NPs offers a potential new avenue regarding the effective use of citrus byproducts.

http://doi.org/10.22401/ANJS.27.5.13
*Corresponding author: medicalphysics2468@gmail.com

1. Introduction

The structural schematic of pectin (as in Figure 1) includes a homogalacturonan (HG) backbone, as well as xylogalacturonan (XGA), rhamno-galacturonan I (RG-I), and rhamnogalacturonan II (RG-II) zones. The core of pectin is composed of acetylated and methylated α (1–4)-galacturonic acid units. The HG zone is the predominant plentiful, 100 GalA units up is the extending and making up about 60% of the pectin. The area of XGA varies since HG due to ß-linked xylose attached at the O-3 position [1].

The RG-I zone of pectin constitutes about 20–35% of its structure besides consists of arabinan and galactan chain segments with OH clusters. These OH sets can be transformed into aldehyde sets in a high-pH environment, giving pectin its reducing properties. This allows RG-I to reduce metal salts to metal nano-forms, facilitating the creation metallic-nanostructd of pectin In contrast, the RG-II zone being a highly complicated segment plus contains rare components like DHA, Kdo, aceric acid, fucose & apiose. This region has been studied for its mitogenic effects and its ability to enhance immune complex clearance.

Metallic nanoparticles (MNPs) are inorganic particles ranging from 3-100 nm in size, composed of refined metals or their derivatives (as in Figure 2). Various types of MNPs have been synthesized using pectin as a diminish agent. Notable examples include: CeO_2 Cu, Au, etc [9, 10].

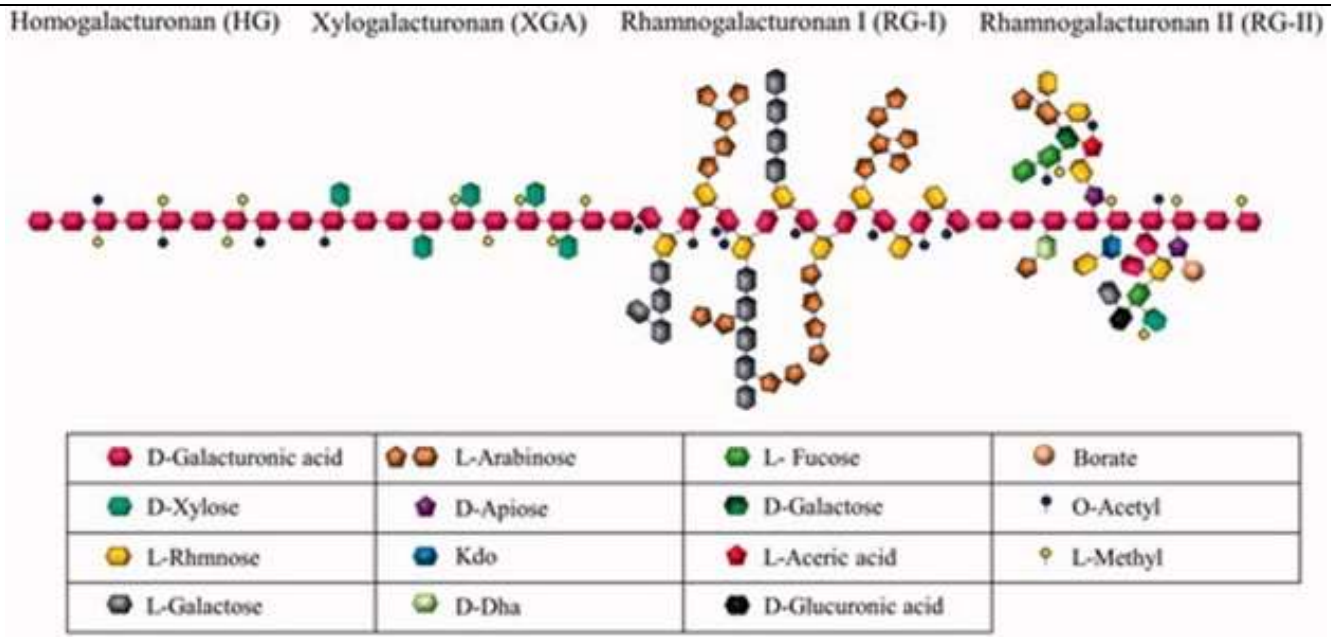

Figure 1: Simplified depiction of pectin segments [1].

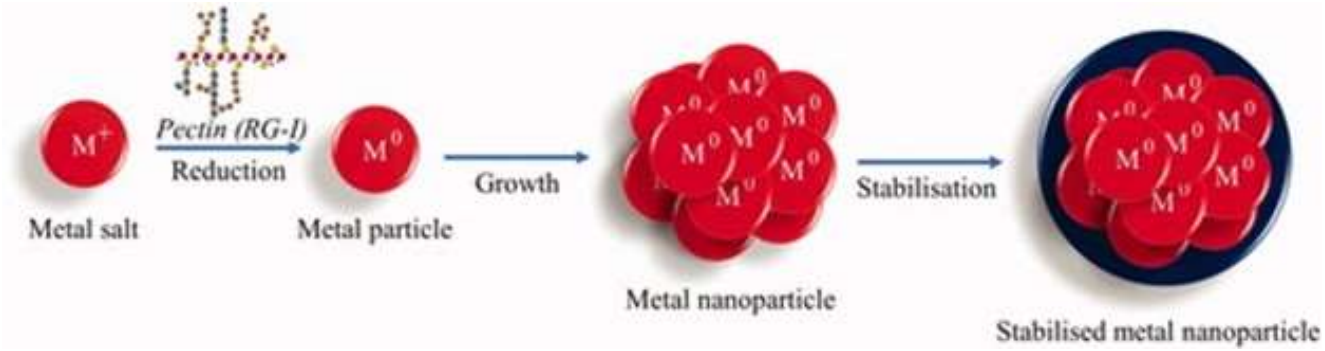

Figure 2: Illustrates the mechanism by which pectin synthesizes metallic nanoparticles [2].

2. Results and Discussion

The diffractogram of Pectin demonstrated a peak that widened at 2θ = 20°, this indicates a reduction in the degree of crystallinity (refer to Figure (3) (a)). Figure 3 (b) and (c) elucidate the XRD patterns of the silver nanoparticles. The peaks were noted at 2θ values corresponding to Ag (111), (200), (220), (311), and (222). The significant intensity at 38° reflection signifies that the crystals are predominantly aligned in this plane. Dorobantu et al. observed that the conversion of Ag from AgO primarily occurs at temperatures below 30°C. The reflections are wider, revealing that the AgNP crystals are smaller. The size of the crystals (t) has been assessed using the Scherrer equation at which the wavelength of diffracted X-ray is represented by λ (1.5418 Å). The average size of the AgNPs was determined to be 20 nm. The most prominent highest intensity at an angle of 32° Aligns with spherically shaped nanostructured pointing to crystallized structure in a face-centered cubic (FCC) structure along the plane (111) of the lattice.

In a Sequence of P-Ag specimen, the assembly of silver nanoparticles (SNPs) relied on both the pectin concentration and the volume of silver ions. The UV-vis spectrophotometer verified that an upsurge in pectin concentration led to a higher absorbance of the specific band at 420 nm that linked to the electron oscillation surface please resonance of SNPs. As the pectin concentration elevated, the reduction efficacy also improved, attributed to the presence of –COOH plus hydroxyl (–OH) functionalities. The UV-visible spectral analysis of the P-Ag samples as illustrated (figure (4)).

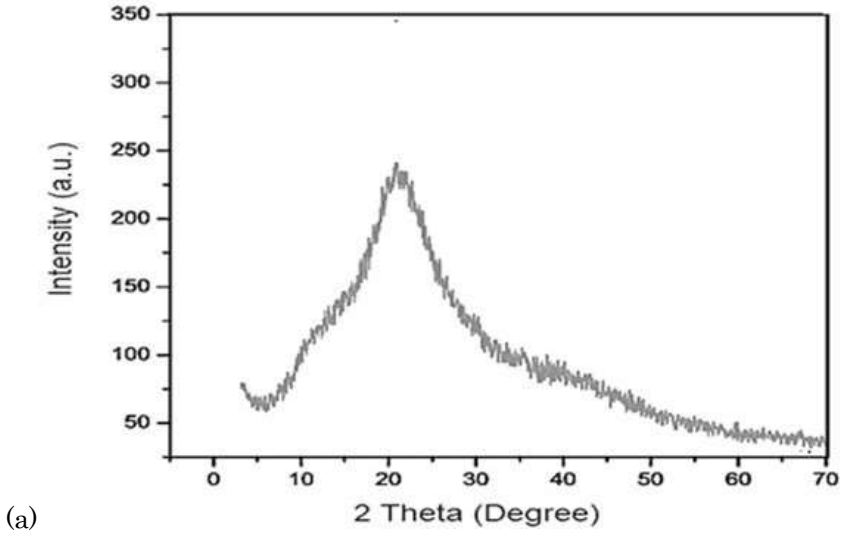

(a)

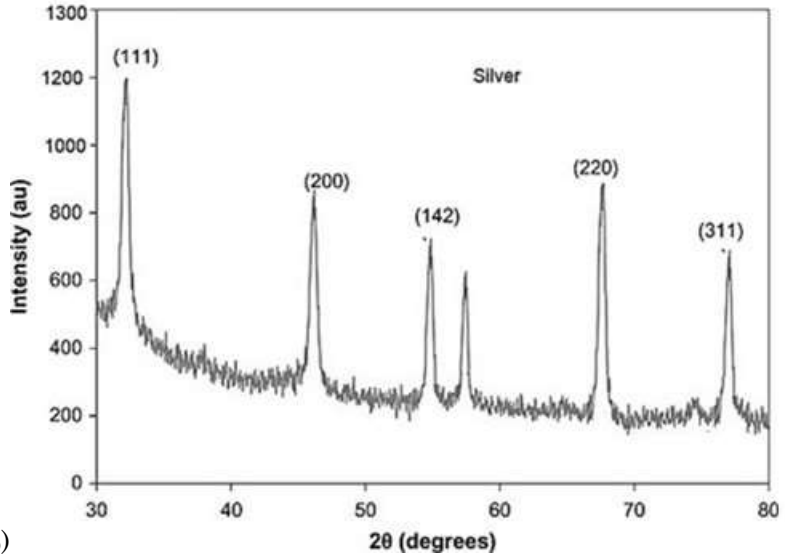

(b)

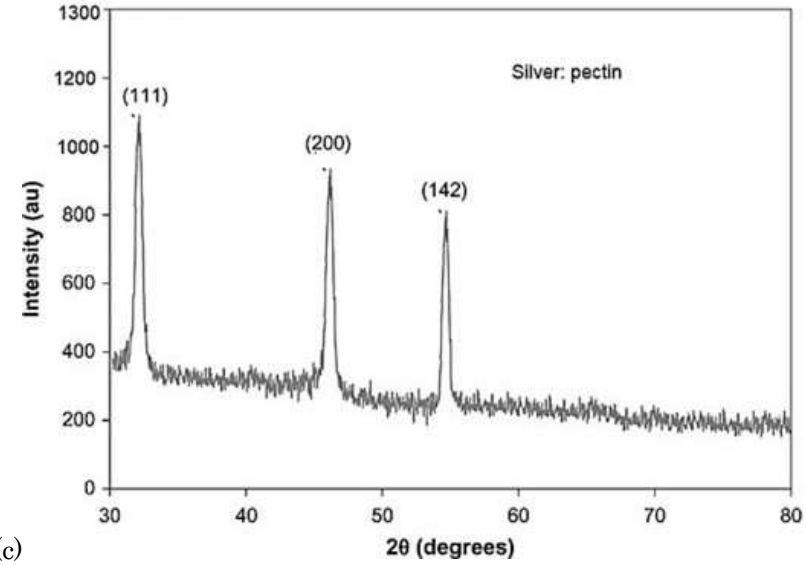

(c)

Figure 3: XRD pattern of (a) pectine (b) AgNPs and (c) AgNPs/pectin.

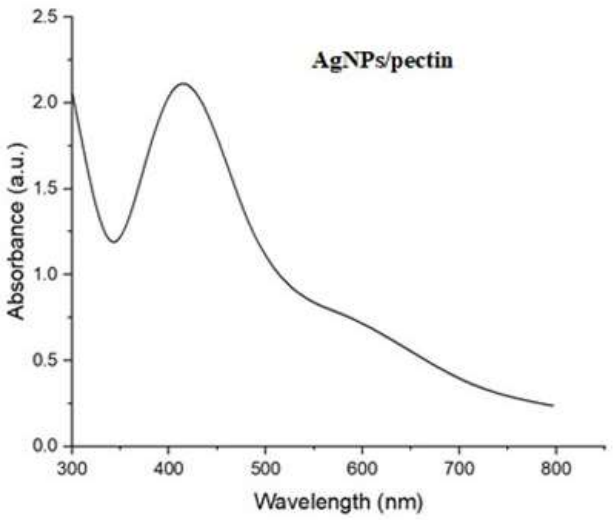

Figure 4: UV–vis absorbance spectrum of Silver/pectin nanostructure.

FTIR spectroscopy is an excellent tool for detecting interactions between silver and Large molecules. Figure (5) depicts the FTIR spectral profiles for P-Ag, alongside the FTIR spectrum of purified pectin, which exhibits distinctive absorption bands at 1588 cm−1 and 3340 cm−1 per cm, corresponding to the Vibrational stretch frequencies of -COO− and –OH groups, correspondingly. The band at 2920 cm−1 is attributed to the -C-H stretching vibration, while the bands around 1416 and 1322 cm−1 are assigned to -CH2 scissoring and -OH bending vibrations, correspondingly. The band at 1019 cm−1 is linked to the [-CH-O-CH2] stretching. In contrast, the FTIR bands of P-Ag display matching attribute signals with slight shifts relating to their oscillation rates (1598 cm−1 for [-COO−], 3256 cm−1 for [-OH], 2948 cm−1 for [-CH2], and 1022 cm−1 for [-CH-O-CH2]). These outcomes strongly indicate the existence of Ag nanoparticles (SNPs) in P-Ag, demonstrating a significant interaction with the pectin polymeric strands.

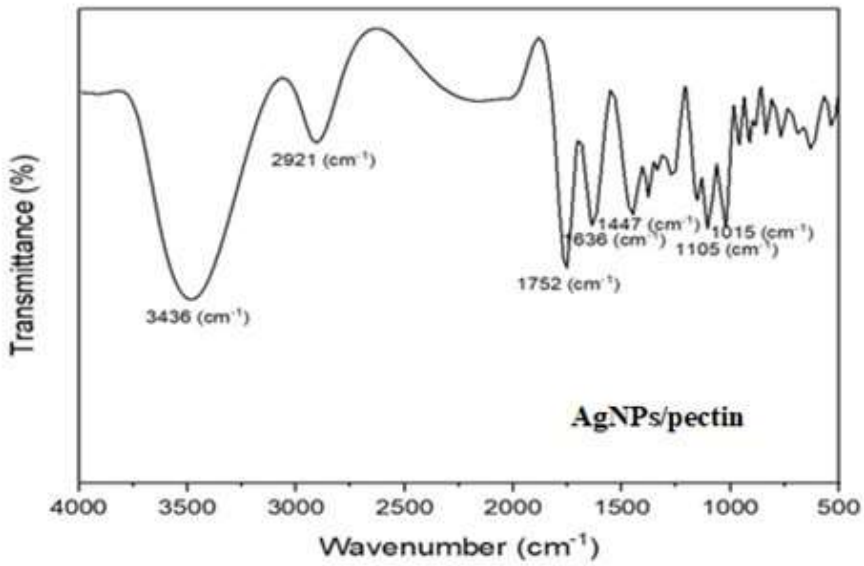

Figure 5: FTIR spectrum of AgNPs/pectin.

The TEM Micrographs of the NMNPs/pectin composites unveiled nanometer-sized structures, showing that the silver nanoparticles (AgNPs) are mostly spherical and evenly spread throughout the observed area. Some AgNPs exhibited irregular shapes, likely due to nanoparticle clustering. The cracks observed in the images are caused by the carbon backing film on the copper grid being damaged as a result of the pectin layer shrinking during dehydration under low-pressure conditions. The pectin film itself cannot be observable in the images, as it is transparent to the electron beam, making it undetectable in the TEM analysis.

Cellular uptake was estimated to show the possible poisonous impact of Ag NPs and Ag: Pectin NPs, their possible penetration, and their accumulation into skin cancer cells. In addition, intensity variation over the incubation period and concentration was evaluated to detect differences in cellular Ag NPs and Ag: Assimilation of pectin-based NPs for the uptake experiments of skin cancer cell line.

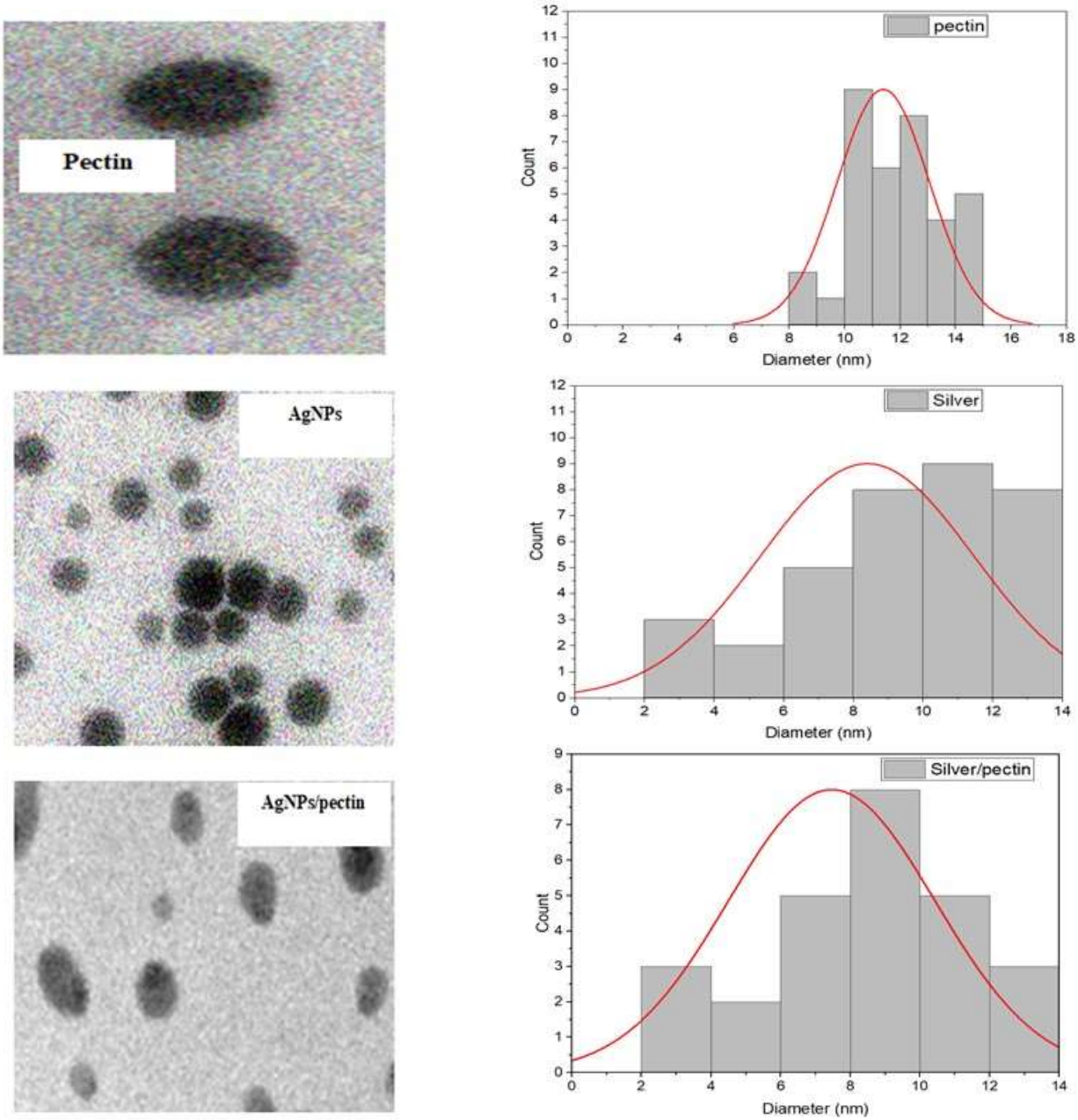

Figure 6: TEM images of AgNPs and AgNPs/pectin.

Incubation periods varied between 0 and 120 minutes, the Ag NPs and Ag:Pectin Nanoparticles were dispersed in the medium at concentrations of 10 mM and 20 mM, alongside a control set of unexposed cells were demonstrated as well as in figure (7) a and b respectively. Figure (7) illustrates that Ag NPs and Ag: Pectin NPs uptake is strongly time-dependent and comparatively speedy. There is considerable assimilation within the first five hours for both Ag NPs and Ag: Pectin NPs. Thus, after five hours, the rate of consumption by skin cancer cells Ag NPs and Ag: Pectin NPs was markedly reduced, reaching stable values at ten hours, indicating that the cell is saturated.

Western blot analysis was used to see if Ag NPs and Ag: Pectin NPs affect cell migration and invasion in skincancer cells. After 24 hours of treatment with Ag NPs and Ag: Pectin NPs, Figure (9) depicts the expression levels of migration- and invasion-related proteins and their corresponding quantitative levels in contrast with the control group (undosed cells) (figure (9)), the relative protein expression in different groups (fold) was lowered after Ag NPs and

Ag: Pectin NPs treatment. Notably, Ag: Pectin NPs treatment resulted in lower protein levels than Ag NPs therapy. Ag: Pectin NPs are more effective than Ag NPs at inhibiting migration and invasion in skin cancer cells. The reason may be to the adhesion of Ag: Pectin NPs on the cell membrane is more than the penetration of it as conformed in cellular uptake results, which means the ability of Ag: Pectin NPs to interact with membrane proteins more than the Ag NPs did. Figure (9) displays the results of western blot analysis of Ag NPs and Ag: Pectin NPs effects on cell migration and invasion. Ag NPs therapy reduced skin cancer cells' migration ability by 60% and Ag: Pectin NPs by 50% when compared to the control group. In addition, the invasive cell rate in skin cell lines was reduced by 30% for Ag NPs and 20% for Ag: Pectin NPs treatment in skin cancer cell lines.

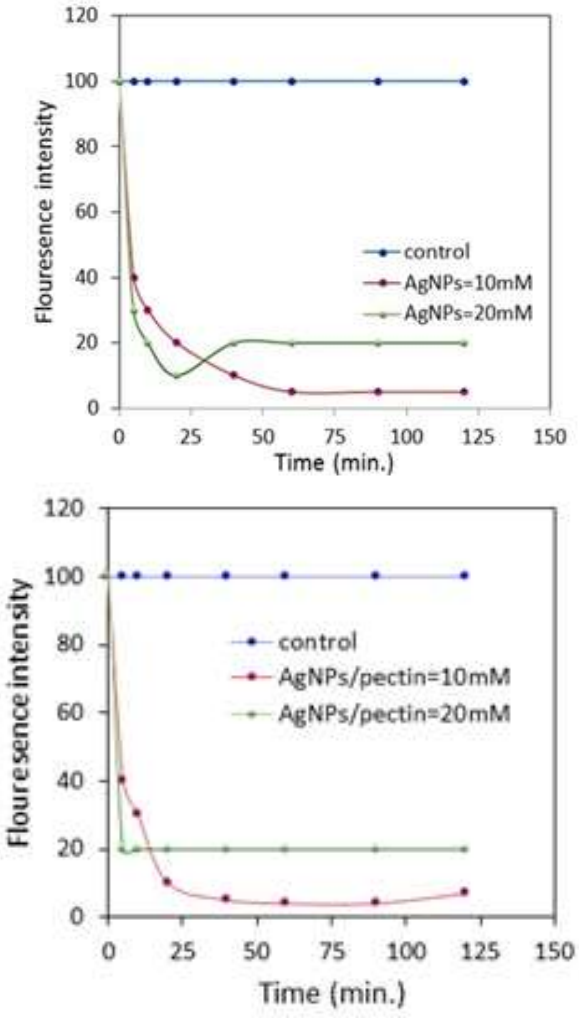

Figure 7: Fluorescence intensity rate as a function of incubation time and concentration of Ag NPs and Ag: Pectin NPs

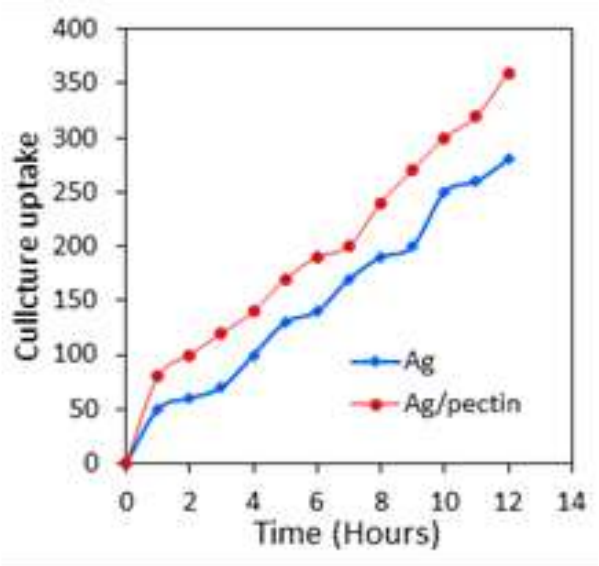

Figure 8.Cellular uptake of Ag NPs and Ag: Pectin NPs

For investigating the possible role of produced Ag NPs and Ag: Pectin NPs as anti-cancer agent on skin cancer cell growth, this is done by evaluating their cytotoxicity [10]. This in vitro evaluation cytotoxicity was performed using the MTT assay on human cancer cell lines and control cell lines (1x10^5 cells per well) at the stage of exponential proliferation. The cells have processed with increasing concentrations of Ag NPs and AgNPs. Cell viability was assessed post one day of experience to varying concentrations of Ag NPs and Ag NPs (6.25, 12.5, 25, 50, 100, 200, and 400 µg/ml). The findings detail the effects of each concentration on cell viability post-treatment are shown in figures (10), and (11), respectively. Additionally, the Half-maximal inhibitory concentrations reading have been determined from data of cell survival rate. The findings in figure (10) designate that AgNPs markedly inhibited skin cancer cell replication varied with dosage ($P < 0.0001$), and The AgNPs solution resulted in a marked reduction in the survival rate of skin cancer cells. At low concentrations of 6.25 and 12.5 µg/ml, the data showed no significance in the cell viability rate between the control and AgNPs groups for skin cancer cells. Ag:Pectin NPs had only insignificant toxicity at concentrations lower than 25 µg/ml despite significant uptake into the cells. The AgNPs set yielded in a significant ($p < 0.05$) decrease in skin cancer cells survival than the control set for at 25 µg/ml and higher concentrations with increasing of cell killing rate attending following progressive order $25 < 50 < 100 < 200$ µg/ml, whereas normal cell had regular viability rate at concentrations from 6.25 to 50 µg/ml and a

significantly lower killing rate at 100-200 µg/ml. Whereas, against normal cells, the cytotoxic activity (IC50) was found to be 60 g/ml and 100 g/ml against normal cells. AgNPs had a greater death rate of 50 percent for skin cancer cells and 20 percent for normal cells when used at a higher concentration of 300 g/ml. Figure (8) illustrate the cytotoxicity yieldings of Ag:Pectin NPs, which showed that Ag:Pectin NPs exhibited cytotoxic effect against skin cancer cell lines in a dose-dependent responding manner. The Ag:Pectin NPs solution resulted in a notable decline in the cell viability rate of skin cancer cells. At particular concentrations, Ag:Pectin NPs had a more negligible cytotoxic effect than those observed with AgNPs. For concentrations from 6.25 to 50 µg/ml, there were no significant differences between the control and Ag:Pectin NPs groups for both the skin cancer cell and normal cells. Denotes that the substantial toxicity in Ag:Pectin NPs was at concentrations higher than 50 µg/ml, despite a significant uptake into the cells. At a concentration of 100 µg/ml and higher, the cell viability was significantly decreased in skin cancer cells with increases in killing rate in each concentration increase. Whereas the normal cell was attended less killing rate at higher concertation of 200 and 400 µg/ml. additionally, it is observed that the cytotoxic effect (IC50) of Ag:Pectin NPs the subjected cells exhibited a higher level of expression up to 195 µg/ml against skin cancer cells and a moderate increase of 250 µg/ml for normal cells. The higher killing rate of Ag:Pectin NPs was at a higher concentration of 400 µg/ml, about 34% for skin cancer cells and 20% for normal cells.

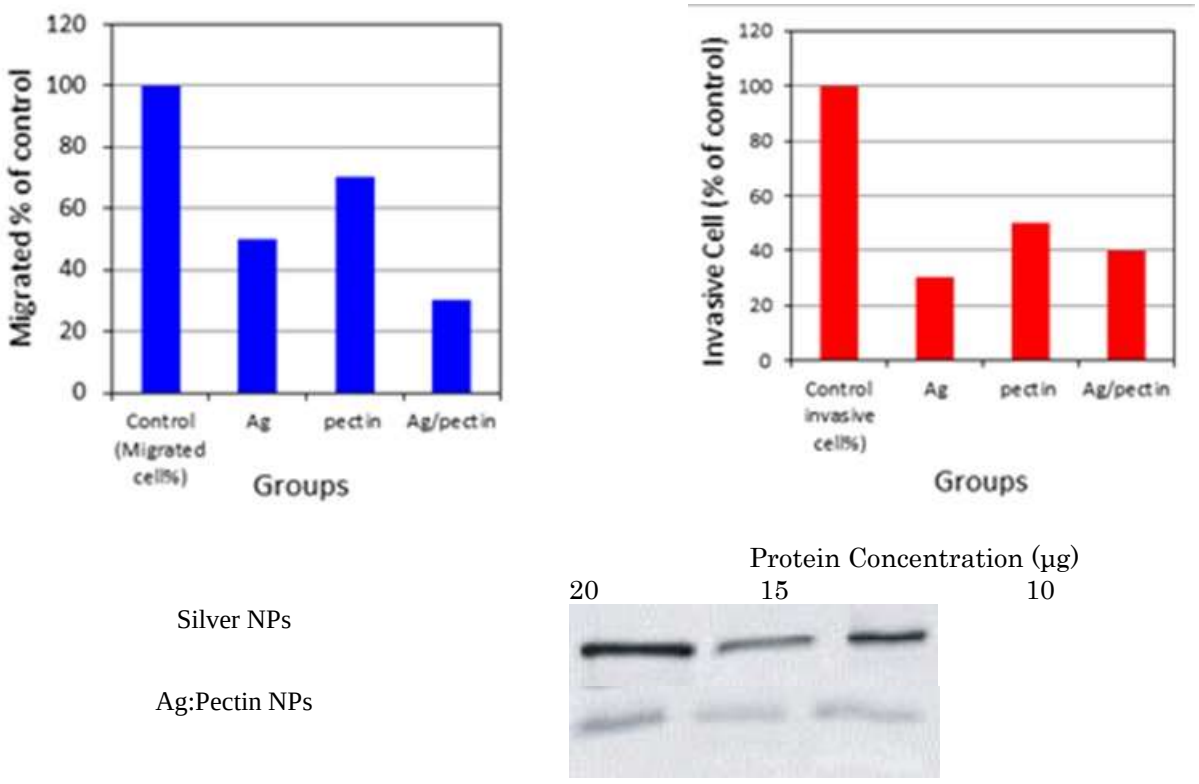

Figure 9: Migration, invasion and Western blot analysis of Ag NPs and Ag: Pectin NPs

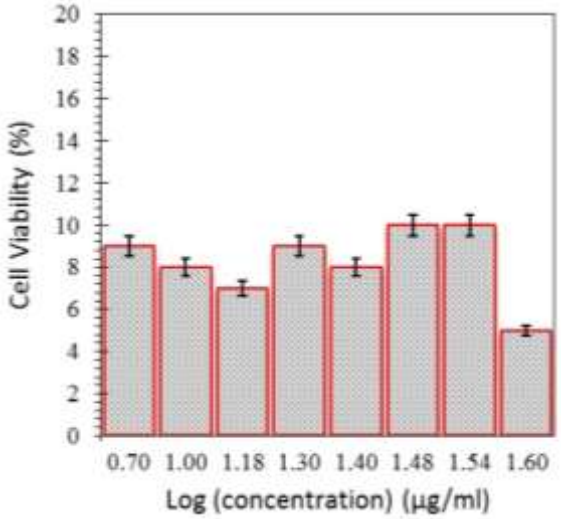

Figure 10: Cytotoxicity analysis of Ag NPs.

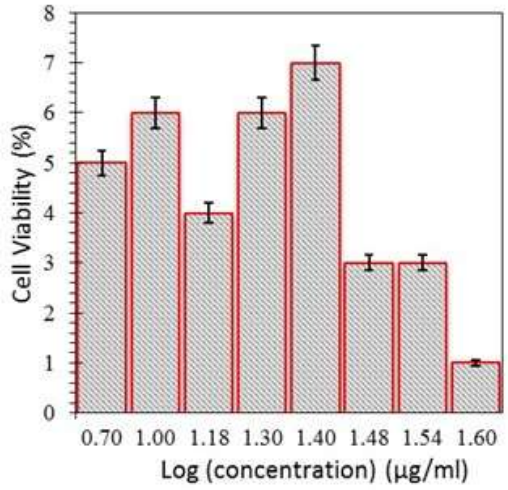

Figure 11: Cytotoxicity analysis of Ag: Pectin NPs

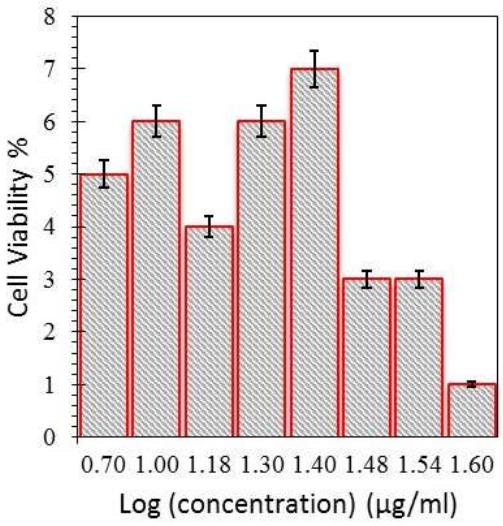

Figure 12: The cytotoxicity analysis of pectin.

3. Conclusions

Based on the preceding findings and discussions, we can draw several conclusions about the investigation directed upon pectin –Ag nanostructured and Pectin-AuNPs. The studies on Pe-AgNPs have shown promising results in antibacterial applications, while Pe-AuNPs have demonstrated significant potential in anticancer and drug delivery roles. Our comprehensive review confirms that Pe-MNPs exhibit notable biological activities, and their biocompatibility and non-toxic nature underscore the suitability of silver (Ag) and gold (Au) as metals synthesized by Pe. Nonetheless, outstanding concerning the relatively limited body of research performed throughout time, there is a need for more extensive studies. Additional research is essential to fully clarify the biological functions of Pe-MNPs through supplementary in vitro and in vivo investigations, along with clinical trials. Such examinations are critical for validating their effectiveness and broadening their potential uses across various sectors. By uncovering the specific physiological impacts of Pe-MNPs, these studies will be fundamental in progressing their application in diverse medical and technological areas.

Conflict of interest: The authors declare no conflict of interest related to this work.

Funding: No finding is received for this work.

References

[1] Bahadar H, Maqbool F, Niaz K, Abdollahi M. 2016. Toxicity of nanoparticles and an overview of current experimental models. Iran Biomed J. 20(1):1–11.

[2] Balachandran YL, Girija S, Selvakumar R, Tongpim S, Gutleb AC, Suriyanarayanan S. 2013. Differently environment stable bio-silver nanoparticles: study on their optical enhancing and antibacterial properties. Plos One. 8(10):e77043.

[3] Baran T. 2018. Pd(0) nanocatalyst stabilized on a novel agar/pectin composite and its catalytic activity in the synthesis of biphenyl compounds by Suzuki-Miyaura cross coupling reaction and reduction of o-nitroaniline. Carbohydr Polym. 195:45–52.

[4] Bhattacharya R, Mukherjee P. 2008. Biological properties of "naked" metal nanoparticles. Adv Drug Deliv Rev. 60(11):1289–1306.

[5] Bobo D, Robinson KJ, Islam J, Thurecht KJ, Corrie SR. 2016. Nanoparticle-based medicines: a review of FDA-approved materials and clinical trials to date. Pharm Res. 33(10):2373–2387.

[6] Borker S, Patole M, Moghe A, Pokharkar V. 2017. Engineering of pectin-reduced gold nanoparticles for targeted delivery of an antiviral drug to macrophages: in vitro and in vivo assessment. Gold Bull. 50(3):235–246.
[7] Borker S, Pokharkar V. 2018. Engineering of pectin-capped gold nanoparticles for delivery of doxorubicin to hepatocarcinoma cells: an insight into mechanism of cellular uptake. Artif Cells Nanomed Biotechnol. 46(Sup2):826–835.
[8] Brandelli A, Ritter AC., Veras FF 2017. Antimicrobial activities of metal nanoparticles. In: Metal Nanoparticles in Pharma. Switzerland: Springer Cham, p. 337–363.
[9] Chen H, Dorrigan A, Saad S, Hare DJ, Cortie MB, Valenzuela SM. 2013. In vivo study of spherical gold nanoparticles: inflammatory effects and distribution in mice. PLoS One. 8(2):e58208.
[10] Daher FB, Braybrook SA. 2015. How to let go: pectin and plant cell adhesion. Front Plant Sci. 6:523.
[11] Das RK, Pachapur VL, Lonappan L, Naghdi M, Pulicharla R, Maiti S, Cledon M, Dalila LM, Sarma SJ, Brar SK. 2017. Biological synthesis of metallic nanoparticles: plants, animals and microbial aspects. Nanotech Envir Eng. 2(1):1–21.
[12] Das S, Chaudhury A, Ng KY. 2011. Polyethyleneimine-modified pectin beads for colon-specific drug delivery: In vitro and in vivo implications. J Microencapsul. 28(4):268–279.
[13] Dash KK, Ali NA, Das D, Mohanta D. 2019. Thorough evaluation of sweet potato starch and lemon-waste pectin based-edible films with nano-titania inclusions for food packaging applications. Int J Biol Macromol. 139:449–458.
[14] Devendiran RM, Chinnaiyan SK, Yadav NK, Moorthy GK, Ramanathan G, Singaravelu S, Sivagnanam UT, Perumal PT. 2016. Green synthesis of folic acid-conjugated gold nanoparticles with pectin as reducing/stabilizing agent for cancer theranostics. RSC Adv. 6(35):29757–29768.
[15] Ghanizadeh A. 2012. Gold nanoparticles and lipoic acid as a novel anti-inflammatory treatment for autism, a hypothesis. J Med Hypotheses Ideas. 6(1):40–43.
[16] Ghorab MM, El-Batal AI, Hanor A, Mosalam FMA. 2016. Incorporation of silver nanoparticles with natural polymers using biotechnological and gamma irradiation processes. BBJ. 16(1):1–25.
[17] Ghozali SZ, Vuanghao L, Ahmad NH. 2015. Biosynthesis and characterization of silver nanoparticles using Catharanthus roseus leaf extract and its proliferative effects on cancer cell lines. J Nanomed Nanotechnol. 6(4):1000305.
[18] Goodman CM, McCusker CD, Yilmaz T, Rotello VM. 2004. Toxicity of gold nanoparticles functionalized with cationic and anionic side chains. Bioconjug Chem. 15(4):897–900.
[19] Hikosaka K, Kim J, Kajita M, Kanayama A, Miyamoto Y. 2008. Platinum nanoparticles have an activity similar to mitochondrial NADH:ubiquinone oxidoreductase. Colloids Surf B Biointerfaces. 66(2):195–200.
[20] Hileuskaya K, Ladutska A, Kulikouskaya V, Kraskouski A, Novik G, Kozerozhets I, Kozlovskiy A, Agabekov V. 2020. Green'approach for obtaining stable pectin-capped silver nanoparticles: Physico-chemical characterization and antibacterial activity. Colloids Surf A Physichochem Eng Asp. 585:124141.
[21] Kawasaki T, Ii M, Kozutsumi Y, Yamashina I. 1986. Isolation and characterization of a receptor lectin specific for galactose/N-acetylgalactosamine from macrophages. Carbohydr Res. 151:197–206.
[22] Khazaei A, Rahmati S, Saednia S. 2013. An efficient ligand-and copper-free Sonogashira reaction catalyzed by palladium nanoparticles supported on pectin. Catal Commun. 37:9–13.
[23] Mohnen, D. (2008). Pectin structure and biosynthesis. Current Opinion in Plant Biology, 11(3), 266-277.
[24] Hileuskaya, K., et al. (2020). Pectin as a reducing agent in the synthesis of metal nanoparticles. Journal of Nanotechnology, 15(4), 543-558.
[25] Tan, S., et al. (2018). Complexity of the RG-II region in pectin: Its composition and biological roles. Carbohydrate Research, 458, 47-57.
[26] Shin, S., et al. (1997). Mitogenic and immune-enhancing activities of pectin. Journal of Immunology, 158(6), 2501-2507.
[27] Sakurai, K., et al. (1999). Effects of pectin on immune complex clearance. Immunology Letters, 70(1), 65-72.